www.czasopisma.pan.pl PAN POLSKA AKADEMIA NAUK www.journals.pan.pl

Arch. Metall. Mater. **64** (2019), 2, 683-694

DOI: 10.24425/amm.2019.127599

H. PAUL*#, M.M. MISZCZYK*, A. GAŁKA**, R. CHULIST*, Z. SZULC**

MICROSTRUCTURAL AND CHEMICAL COMPOSITION CHANGES IN THE BONDING ZONE OF EXPLOSIVELY WELDED SHEETS

In this work, the effect of heat transfer during explosive welding (EXW) and post-processing annealing on the microstructural and chemical composition changes have been thoroughly analysed using scanning and transmission electron microscopies and X-ray synchrotron radiation. Several combination of explosively welded metal compositions were studied: Ti with Al, Cu with Al, Ta or stainless steel, stainless steel with Zr or Ta and Ti with carbon steel. It was found that the melted metals exhibit a strong tendency to form brittle crystalline, nano-grained or even amorphous phases during the solidification. For all analysed metal combinations most of the phases formed in the zones of solidified melt do not appear in the equilibrium phase diagrams. Concurrently, the interfacial layers undergo severe plastic deformation forming nano-grained structures. It has been established that these heavily deformed areas can undergo dynamic recovery and recrystallization already during clad processing. This leads to the formation of new stress-free grains near the interface. In the case of low temperature and short time post processing annealing only the melted zones and severely deformed layers undergo recovery and recrystallization. However, drastic changes in the microstructure occurs at higher temperature and for longer annealing times. Applying such conditions leads to diffusion dominant processes across the interface. As a consequence continuous layers of intermetallic phases of equilibrium composition are obtained.

Keywords: explosive welding, SEM and TEM, multilayered clads, reactive metals, amorphous and nano-grained phases

1. Introduction

The optimization of plate cladding should be based on a detailed understanding of microstructural and chemical composition changes in the bonding zone. This becomes extremely important for bi- and multi-layered clads manufactured by explosive welding (EXW) technology since their mechanical and functional properties are strongly affected by structural and chemical changes in the interface regions. This can be efficiently tailored not only by bonding parameters [1-4] such as detonation velocity [5-8] and stand-off distance [5,9,10] but also upon post-processing heat treatment e.g. [12,13].

The plasma jet formed at the collision point/line together with impact energy and large plastic work, produce a considerable temperature increase leading to local melting during EXW [14-18]. Simultaneously, the shear strains/stresses, which occur due to oblique collision of the plates are responsible for strain hardening and circular material displacement in layers near the interface. High temperature and shear stresses cause also a turbulent flow of layers near the interface. This leads to the formation of wavy interfaces of the joined sheets. The process of fast heating followed by fast cooling [14,16] leads also to remarkable microstructural changes in near-the-interface layers of the bonded plates. Since the interfacial layers undergo severe plastic deformation (with a pronounced increase of dislocation density and extremely strong grain refinement, e.g. [14-18]) they appear to undergo recovery or/and recrystallization. Moreover, the rapid cooling of the order of 10^4-10^5 K/s is sufficient for the formation of a martensitic structure [14]. Such a phase transformation was recently presented by Bataev et al. [14] in carbon steel to carbon steel composite. It becomes increasingly apparent that above phenomena determine strongly the mechanical and several physical properties of the clad. It is also relatively well-documented that the wavy interfaces produce usually a better mechanical bonding in comparison with flat semi-melted interfaces [1,2]. However, if the quantity of melted zones is too large it can exert a detrimental effect on the strength of the bimetal through micro-/macro- cracks formation [19]. Scanning electron microscopy observations revealed that large zones of the solidified melt can also modify the structure of parent plates due to heat transfer. It may encourage recovery and recrystallization processes of severely deformed regions leading to local softening.

On the other hand, during post-processing annealing the structure of EXW clads can be easily modified by formation of new layers composed of intermetallic phases. After EXW process various types of changes are observed in layers near the interface of EXW clads due to applied annealing conditions

* INSTITUTE OF METALLURGY AND MATERIALS SCIENCE, POLISH ACADEMY OF SCIENCES, KRAKOW (POLAND)
** ZTW EXPLOMET, OPOLE (POLAND)
# Corresponding author: h.paul@imim.pl

(temperature/time). It is expected that the diffusion processes are dominant across the interface for high (and very high) annealing temperatures (as compared to the melting points of joined materials) and for longer annealing times. However, it seems that the diffusion control mass transfer does not play any decisive role during EXW. This opens the possibility to fabricate materials of laminar structure with significantly improved strength properties.

Therefore, the purposes of the present work is to analyse the effect of heat transfer on the microstructural changes in layers close to the interface during both EXW and post-processing heat treatment. For these reasons, we provide complex analyses of the microstructure and the chemical composition changes within the melted zone and within the parent metal layers directly adjacent to the interfaces of explosively welded sheets. The analysis is provided by means of transmission (TEM) and scanning (SEM) electron microscopy.

2. Experimental

EXW of each material compositions was performed by High Energy Technologies Works 'Explomet' (Opole, Poland). The welding conditions were tailored through the parallel geometry route with various intensity of explosive load and stand-off distances depending on materials combination and sheets thickness. The sizes of the sheet/plates were ~150 × 250 mm^2 with varying thickness, as presented in Table 1. The contact surfaces of the joined sheets/plates were grounded, cleaned of solid particles and degreased. A detonator was located in the middle of the shorter edge of the flyer plate. The annealing temperatures varied between 550°C and 700°C depending on the clad compositions with annealing times up to 1000 h.

TABLE 1

The thickness of sheets/plates used for clads preparation

No.	Metals composition (upper/bottom)	Sheet/plate thickness	
		Upper sheet/plate (mm)	Bottom sheet/plate (mm)
1.	Zr700/stainless steel	3.15	18
2.	Zr700/carbon steel	3.15	20
3.	Ti/carbon steel	2	13
4.	Ta/stainless steel	2	30
5.	Ta/Cu	2	6
6.	Ti/Cu	3	3
7.	Ti/Al	1	1
8.	Cu/stainless steel	3	5
9.	Cu/Al	8	30

Samples for SEM and TEM analyses were cut-off from the properly bonded clads. The observation plane was perpendicular to the transverse direction (TD) both for initial and heat treated samples. All welds were characterized by good mechanical properties since the strength of the weld was higher than the strength of the weaker component. The sample edges were parallel to the RD and parallel to the jetting direction and to the normal direction (ND). The nano-/micro- scale microstructure observations and the chemical composition measurements were performed using a FEI Technai Super TWIN G^2 FEG (200kV) microscope equipped with a high-angle annular dark field scanning/transmission detector (HAADF/STEM) and an energy dispersive X-ray (EDX) microanalyser. The beam diameter applied was ~1 nm. The FEI Quanta Focus Ion Beam (FIB) cutting was applied for the thin foil preparation along the ND/TD section. The global microstructural analyses were performed by means of SEM, with the use of SEM – FEI Quanta 3D combined with an EDX and electron backscattered (EBSD) detectors. In order to perform phase analysis near the interfaces upon EXW and after post-processing annealing, high resolution X-ray diffraction (XRD) measurements with synchrotron radiation were carried out using a HZG beamline (P07B) located at PETRA III (electro storage ring operating at energy 6 GeV with beam current 100 mA) at DESY, Hamburg, Germany [20].

3. Results

Various combinations of metals were explosively welded in order to estimate the influence of chemical composition on the phase transformation and morphology of the melted zone. All the clads analysed in this work can be divided into the following groups:

i. Combinations of metals and alloys that form mixed amorphous and nano- grained melt zones such as: Zr700 alloy with carbon steel – P355JN (CS) or stainless steel – 10CrMo9-10 (SS), Ti (Gr.1) with carbon steel – P355JN, Ta (99.9%) with stainless steel – 10CrMo9-10 and Ti (Gr.1) with Cu-DHP.
ii. Combinations of metals and alloys that form nano- grained melt zones for instance: Al (AA1050) with Ti (Gr.1) and Cu-DHP with stainless steel – 10CrMo9-10.
iii. Combinations of metals and alloys that form fully crystalline structures of melted zones. To this group belongs Al (AA1050) /Cu-DHP clads.

3.1. Heat influence during explosive welding. Structure and chemical composition of large melted zones

At the macro-/meso-scale, all the interfaces were outlined by a characteristic sharp transition indicating that there was no mechanical mixing between the welded metals in the solid state. The areas of different chemical composition are usually randomly distributed in the melted zones but in some places a specific swirl-like distribution of elements is revealed. Thus, the latter experimental observation of elements distribution in the melted zone describes the vortex formation mechanism more correctly than the jet-trapping mechanism mentioned by Crossland [2]. For all alloy combinations the morphology of the joints was characterized by wavy patterns, as presented in Fig. 1 for

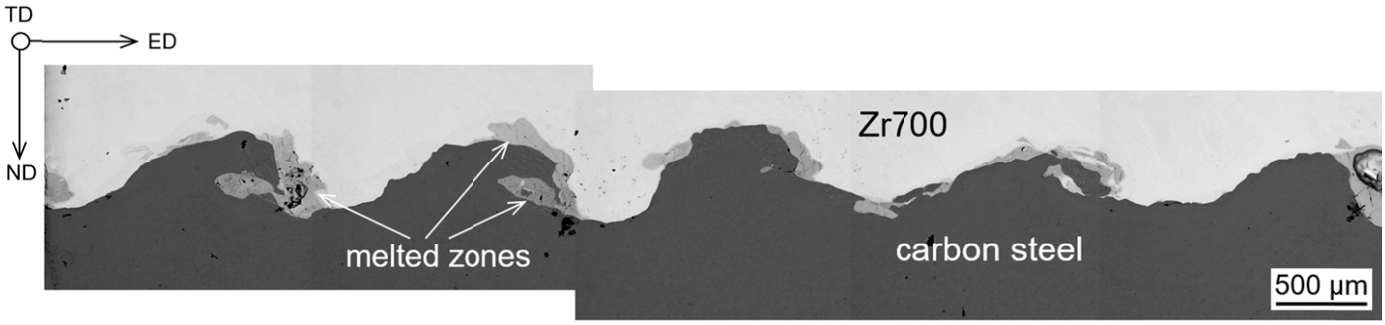

Fig. 1. SEM/BSE image showing typical wavy interface with solidified melt areas of Zr700/carbon steel clad

the Zr700/carbon steel clad. Large melted zones (intermetallic inclusions), if present, were preferentially located near the front slope of the waves or within the vortexes of waves. In some cases, the network of macro-/micro- cracks within the brittle intermetallic inclusions were observed; they were always limited to the melted zone. The macro-cracks were mostly situated perpendicularly to the interface, whereas an additional network of micro-cracks was non-regular and observed only at SEM scale. It is important to note that extremely thin melted zones were observed in all analysed clads. Such a thin layer can be easily overlooked with optical microscopy or even at low magnification SEM observations. However, using TEM the presence of continuous layer was indisputably proved. Its thickness was usually few tens of nanometers. This layer of the solidified melt was completely free of any cracks. Microstructures of solidified melt zones in different metal compositions are discussed in detail below.

3.1.1. Explosive welding of Zr700 to stainless steel

Zirconium provides excellent corrosion resistance to various corrosive environments. Therefore, Zr700/stainless steel bimetals are widely used in the chemical industry for chemical reactors manufacturing. Figures 2a-c show SEM/backscattered electrons (BSE) and TEM/bright field (BF) images illustrating the microstructures near the interface of the Zr700 to stainless steel. The structure of the melted zone is composed both of amorphous and ultra-fine crystalline phases. The crystallization process dominates in the areas at both interfaces, whereas the nucleation of new grains in the interior of the solidified melt zone is less frequent. The new crystallites, which nucleate from the amorphous phase, are of different size, usually ranging between 20 nm and 80 nm. They were observed as single isolated grains 'plunged' in the solidified melt or as compact chains of grains, as earlier observed for the Zr700/CS clads [16]. The chemical composition of the phases formed within the zones of solidified melt was strongly diversified and the most of them often far from the phases observed in the equilibrium phase diagram. In the analysed areas the Zr content changed within a broad range, from about 25 at.% to 75 at.%. However, the areas of chemical composition close to the phases present on the equilibrium Fe-Zr phase diagram were also observed. It is interesting to note that despite intense mixing in the molten or semi-molten state the phases enriched in Zr were usually observed close to the Zr700 plate (e.g. $Fe_{21.8}Zr_{75.0}Ni_{1.8}Cr_{1.4}$), whereas the ones enriched with Fe – close to the stainless steel plate (e.g. $Fe_{72.0}Zr_{26.4}Cr_{1.6}$).

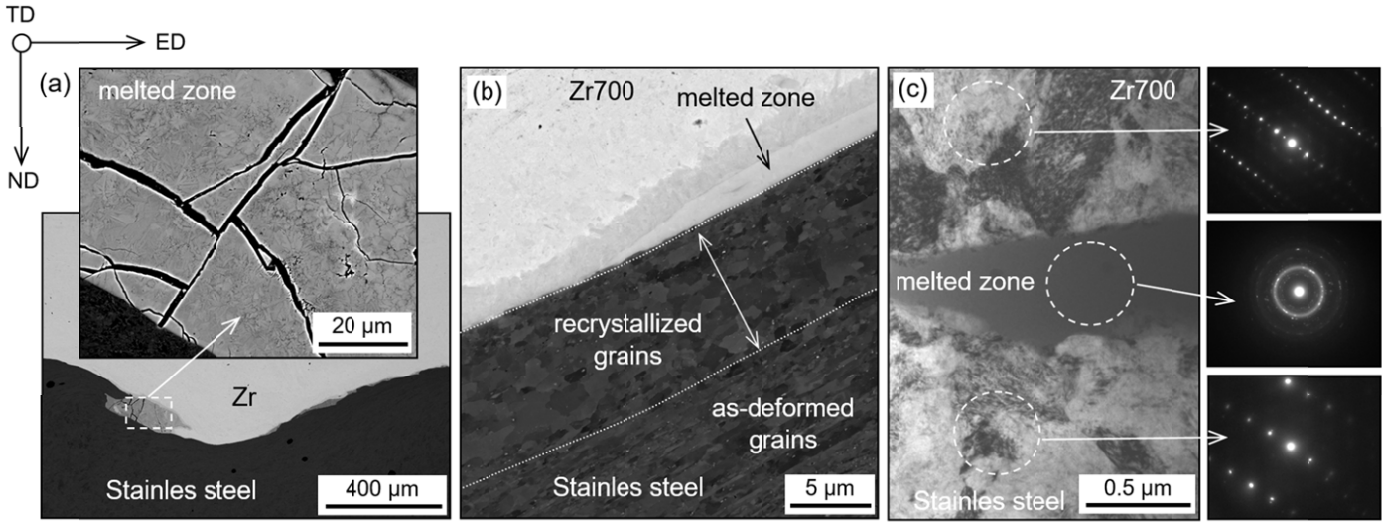

Fig. 2. Structure of melted zone and layers near the interface in the Zr700/stainless steel clad. (a) Solidified melts formed near the wave crest and their internal structure with network of macro-/micro- cracks. (b) Recrystallization of the severely deformed structure of carbon steel in the areas adhering to the interface. (c) Morphology of thin solidified melt zone. (a, b) SEM/BSE and (c) TEM/BF imaging

3.1.2. Explosive welding of Ti to carbon steel

Ti/carbon steel metals combination is the most produced commercially clads. A typical interface between Ti(Gr1) and carbon steel is shown in Fig. 3a. This SEM/BSE image showing a wavy character of the interface. The melted zones were situated at the crests of the wave and inside the wave vortexes. It can be seen that internal structure is composed of very fine grains with the diameter ranged mostly between 150 nm and 200 nm (Figs. 3b, c). Generally, the grains showed a typical crystalline contrast during tilting in TEM. Interestingly, certain grains resemble small dendrites. However, amorphous areas are also observed. This can be deduced from the well-marked ring on diffraction pattern in Fig. 3d, being consist with earlier works e.g. by Song et al. [18] in carbon steel to Ti clad. The chemical composition of the phases that form within this intermetallic layer can be usually described by various chemical compositions – $Fe_{(0.25\text{-}0.67)}Ti_{(0.33\text{-}0.75)}$. However, some areas of chemical composition close to the Fe_2Ti_3 equilibrium phase were also observed inside the melted zone. Thus, in the Ti/carbon steel system amorphous and nano- grained melt zones can be observed.

3.1.3. Explosive welding of Cu to Ti

This composition is often used in electrotechnical applications. Typical large melted zones have been formed inside the wave vortex (Fig. 4a) and on the crest of the wave (Fig. 4b). The internal microstructure of the solidified melt zones is composed of mixture of amorphous areas, small equiaxed grains (the diameter of these grains ranged from 0.1 to 1.0 μm) and columnar grains but a thin layer of solidified melt is composed only of amorphous and nano-grained phases (Fig. 4c). In some cases the complex force interaction during the clad formation pushes locally the solid material into the liquid or semi-liquid material. This leads to the situation, where the parent material (Cu or Ti) is occasionally enclosed inside the solidified melt. Similar observation was made by Fronczek et al. [12] in Ti/Al and Paul et al. [17] in Ta/stainless steel clads, where islands of higher melting point metal (Ti or Ta, respectively) were enclosed within solidified melt inclusions. Despite the fact that most of the phases do not appear in the equilibrium Cu-Ti phase diagram, they can be found areas with chemical compositions corresponding to all possible equilibrium phases, like: Cu_4Ti, Cu_2Ti, $CuTi$, $CuTi_2$, Cu_3Ti_2 and Cu_4Ti_3.

3.1.4. Explosive welding of Ta to stainless steel

Ta/stainless steel clads are used in the chemical or pharmacy industry. Tantalum provides excellent corrosion resistance, while the stainless steel substrate is typically used as a load bearing component. The volumes inside the intermetallic inclusions can be fully amorphous, crystalline, or their internal structure

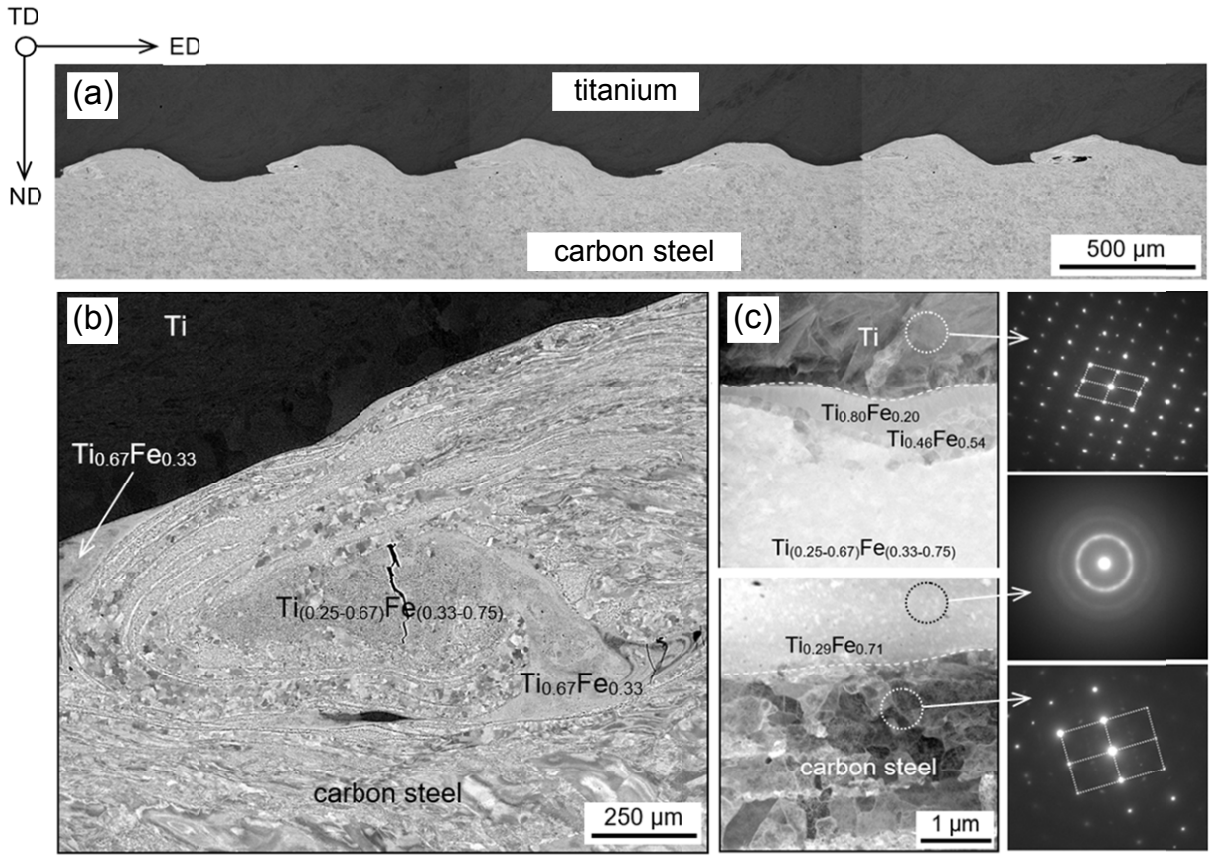

Fig. 3. (a) Interface waviness in Ti/carbon steel clad. (b) Structure of severely deformed layers of carbon steel on the wave crest and the zone of solidified melt enclosed inside the wave vortex. (c) Morphology of solidified melt zone. (a, b) SEM/BSE and (c) TEM/BF imaging

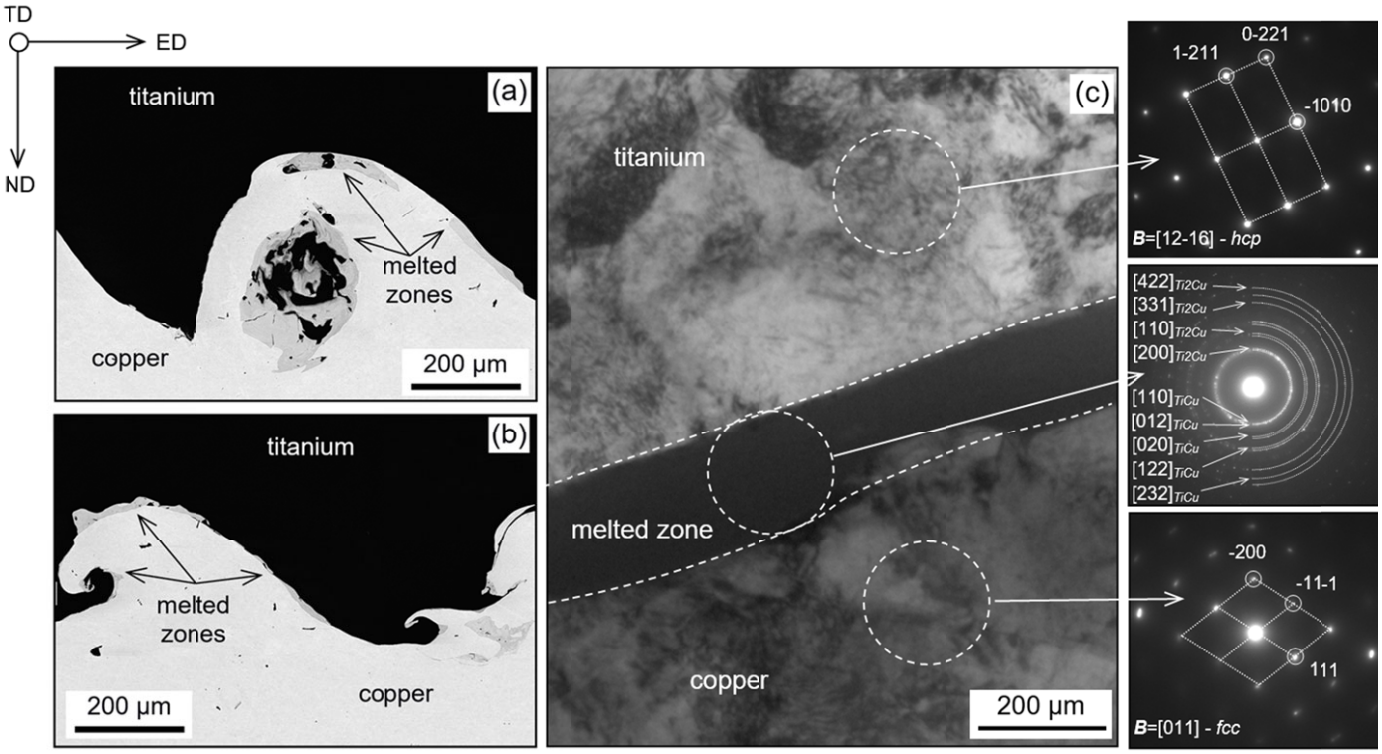

Fig. 4. Structure of interfacial layers in Ti/Cu clad. Typical large melted zones formed: (a) inside the wave vortex and (b) on the wave crest. (c) The structure of the thin layer of the solidified melt and the structure of parent plates near the interface. (a, b) SEM/BSE and (c) TEM/BF imaging

can be a mixture of nano-crystalline and amorphous phases. In some cases, the new grains that nucleate within the solidified melt take the form of dendrites, with a well-developed core and arms (Fig. 5a, b). In the case of melted zones situated on the wave crest their internal microstructure show alternating BSE contrast being an evidence for strong chemical composition changes inside the zone (Fig. 5a). The areas of similar contrast reveal rotational character of the elements distribution due to intensive stirring of the materials in the liquid and/or semi-liquid states. This is also confirmed by SEM/EDX element mapping taken from the same area, as presented earlier in [17]. In the case of the thicker melted zones situated at the wave crest or inside the wave vortexes, the local composition is strongly place dependent due to intense mixing in liquid or/and semi-liquid states. For extremely thin melted zones the morphological and chemical composition changes can be directly related with distance from the parent plates. For all analysed cases an amorphous layer is adhering to the Ta sheet (Figs. 5c, d), whereas the layer adhering to the steel is crystalline. The chemical compositions of particular layers were different and most of the observed phases were far from equilibrium one, i.e. the phases were not observed in the equilibrium phase diagram. The TEM/EDX measurements showed (Fig. 5c), that inside the continuous layer the distribution of particular chemical elements is similar to those observed during stationary conditions, i.e. the layers of the solidified melt situated closer to SS plate were enriched with Fe, Cr and Ni. Accordingly, the concentration of Ta near the Ta sheet was larger as compared to layers that are more distant.

3.1.5. Explosive welding of Ta to copper and copper to stainless steel

Despite the fact that it is relatively easy to join Ta to stainless steel using EXW technology, there are serious difficulties with 'conventional' welding of Ta/stainless steel clads during further processing. Therefore, an intermediate layer, usually made of soft material and high thermal conductivity such as Cu, to joint two plates is used. In such a configuration the melted zones close to the Ta/Cu interface consists of a mechanical mixture of Cu and Ta particles of different sizes (Figs. 6a, b). The spherical particles of Ta are homogeneously distributed in the Cu matrix and no metastable phases were observed, independently of the scale of observation.

Figure 6c shows the zone of solidified melt at the Cu stainless steel boundary observed at SEM scale, whereas Figs. 6d, e show their internal structure observed at TEM scale near both interfaces, i.e. Cu/melted zone and melted zone/stainless steel. What can be seen is a different morphology of grains that nucleate near both interfaces. Especially apparent are characteristic sublayers composed of small columnar grains near the Cu plate. This indicates a more effective heat transfer across this interface compared to other side of melted zone.

3.1.6. Explosive welding of Ti to Al

Multi-layer composites based on low density metals are especially attractive for mechanical engineering, e.g. aircraft

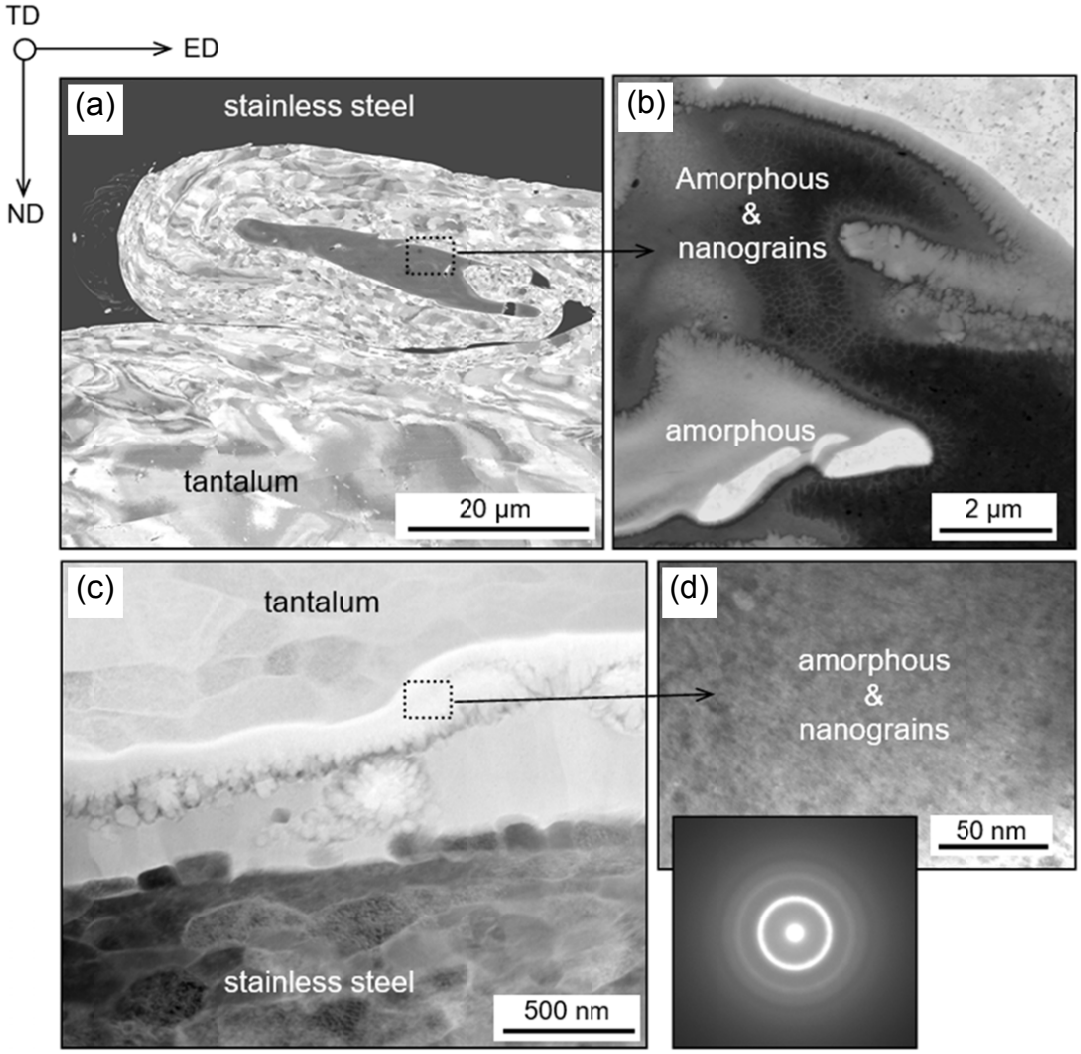

Fig. 5. (a) Layer near the interface in Ta/stainless steel clad with the zones of solidified melt inside the wave vortex and on the wave crest. (b) Internal structure of the solidified melt zone showing mixture of amorphous and nano-grained phases. (d) Structure of thin layer of solidified melt between parent plates and amorphous sublayer directly adhering to the Ta plate. (a, b) SEM/BSE and (c, d) TEM/BF imaging

industry or aerospace applications. Regarding large zones of the solidified melt (Fig. 7) its internal microstructure shows strong chemical composition changes inside the zone during clad formation. The SEM/EDX analyses showed that metastable phases dominate rather the structure of large melted zones while the equilibrium phases were observed rarely. The chemical composition of these phases varies between 20-80 at.% both for Ti and Al. Additionally, the above results indicate a wide spectrum of intermetallic phases with a chemical composition very close to Al_3Ti, Al_2Ti, AlTi, $AlTi_2$, $AlTi_3$. In the case of thin melted zones the chemical composition can be directly related to the AlTi or Al_2Ti equilibrium phases. The TEM/BF images and selected area diffraction patterns, shown in Fig. 7e, confirmed that the melted zones exhibit mostly a ultra-fine-grained structure.

3.1.7. Explosive welding of Al to Cu

The Al/Cu clads is the only one system, in which the melted zones are fully composed of crystalline phases. They occur mostly in the form of dendrites. The micrographs presented in Fig. 8 were obtained from a thin foil cut-off from the sample area containing intermetallic zone of about 10 µm thick placed on the crest of the wave. However, near the flat part of the interface, a very thin (even below 50 nm) intermetallic interlayer was always observed, as presented earlier in [15]. The bright-field TEM image (Fig. 8b) shows a typical microstructure across the whole thickness of the solidified melt layer and the areas of parent sheets adhering to the interfaces. The analyses performed by means of TEM showed a strong variability in the chemical composition inside the layer. Most of the phases were not observed in the equilibrium Cu-Al phase diagram, with the copper concentration ranged between 33at.% and 67at.%. However, a closer TEM inspection revealed certain areas with chemical composition close to three equilibrium phases of Al_4Cu_9, AlCu and Al_2Cu, which always showed a typical crystalline contrast during tilting in TEM. Some of the grains within the melted zone resemble dendrites (Fig. 8b). The diameter of these grains ranged between 0.5 µm and 2 µm.

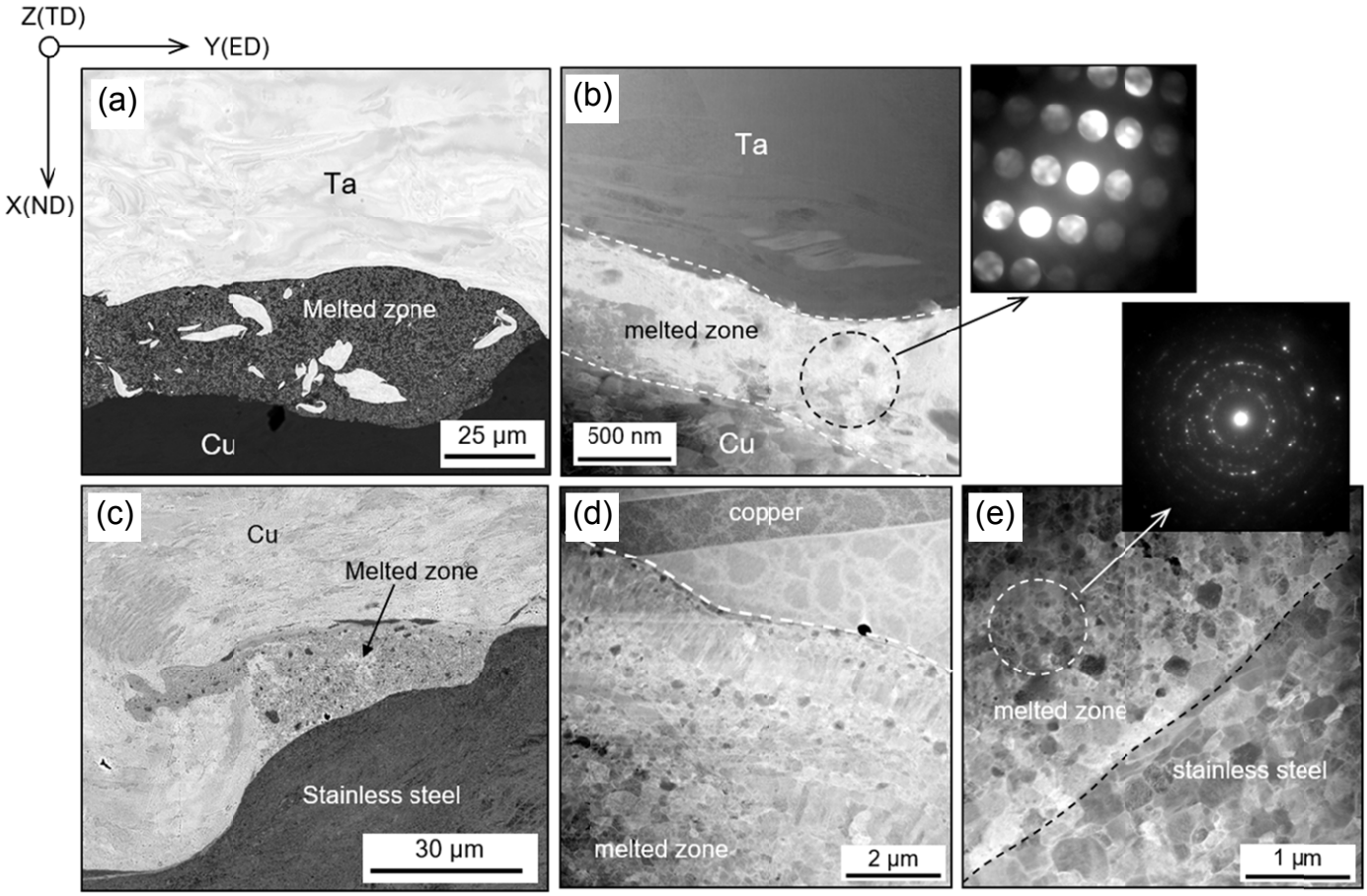

Fig. 6. Structure of melted zone in the Ta/Cu/stainless steel clad. (a) SEM/BSE and (b) STEM/HAADF images showing the melted area near the Ta/copper interface. (c) Nano-grained structure of the solidified melt zone at the copper/stainless steel interface – (c) SEM/BSE and (d, e) STEM/HAADF images showing the structure of melted area

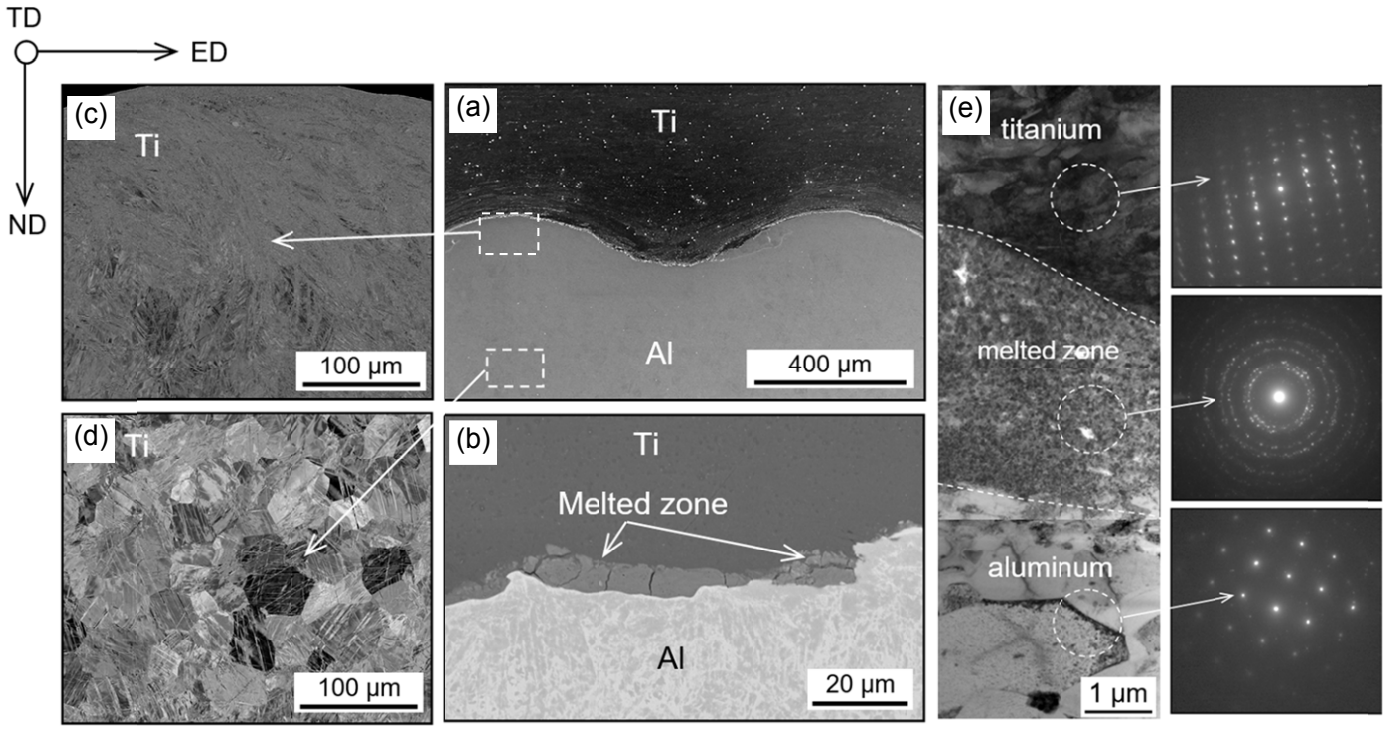

Fig. 7. Layer near the interface in the Al/Ti clad. (a) Wavy structure of Al/Ti interface, (b) semi-continuous melted zone, (c) intense twinning in Ti near the wave crest, and (d) bottom part of the wave. (e) Internal structure of the melted zone. (a-d) SEM/BSE and (e) TEM/BF images

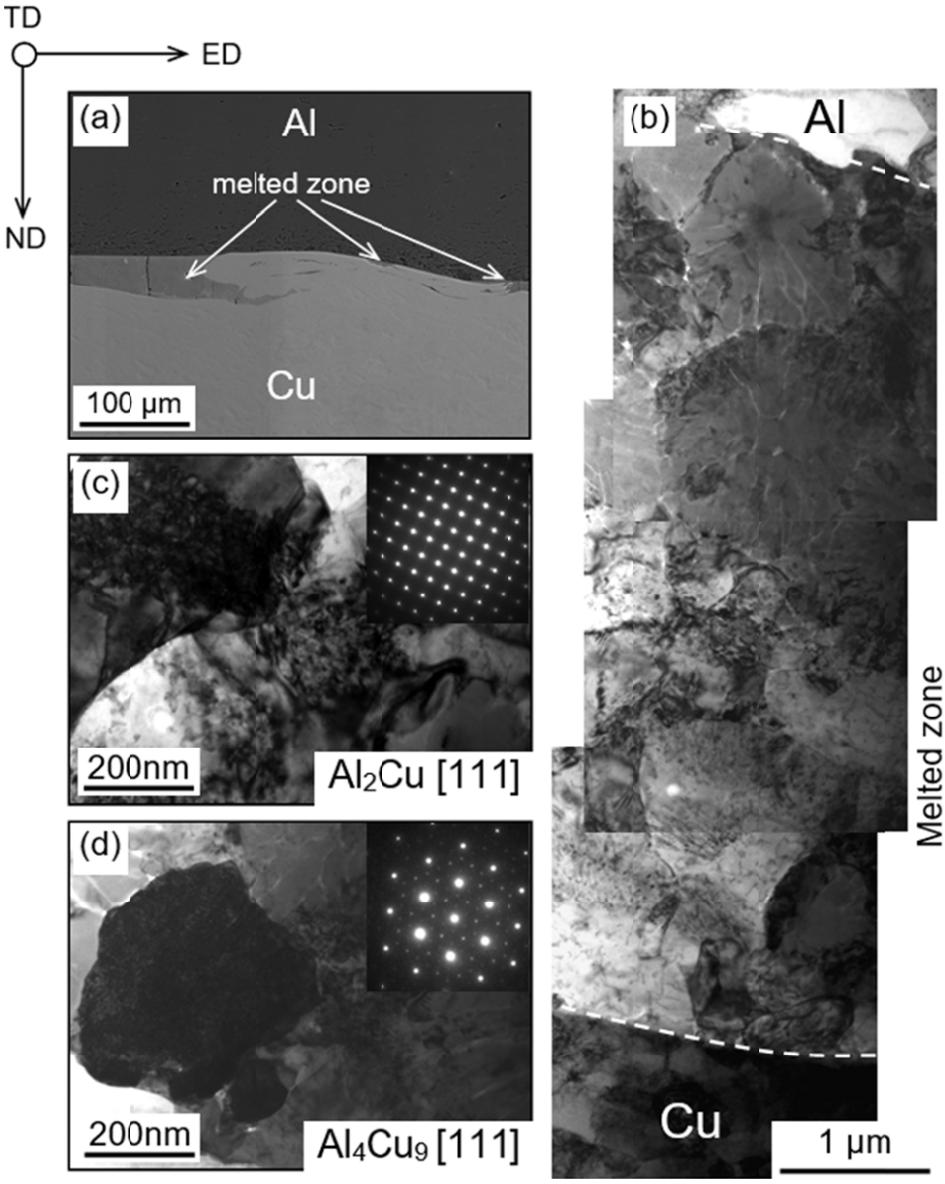

Fig. 8. Structure of melted zone in the Al/Cu clad. (a) Crest of the wave with large melted zone. (b) Dendritic structure of the melted zone, (c) formation of the Al_2Cu and Al_4Cu_9 phases. (a) SEM/BSE and (e) TEM/BF images

3.2. Microstructure of severely deformed layers near the interface

The microstructure evolution of the parent sheets/plates strongly depends on the competition between strain hardening and softening processes. It has been established that an intense shearing in the near-the-interface layers of both plates leads to a strain hardening due to the increase of structural defects. The width of this strain hardened layer strongly depends on the material. Beside slip the twin deformation mode is often observed especially when it comes to *hcp* structures (Figs. 7c, d). As usually slip precedes twinning – very thin deformation twins with dislocation cell structure can be detected in Cu/Al or Al/Ti clads, in Cu and Ti sheets, respectively.

Dynamic recovery and recrystallization are typical processes leading to softening and important microstructural changes in the parent sheets. However, precise analysis of dynamic recrystallization and recovery is exceptionally complicated as both phenomena strongly depend on the melting point of joined metals, temperature and strain. Moreover, in very fast processes the effect of strain rate have also to be considered. Deformation processes usually predominate softening ones in areas near the interface of parent sheets containing a very thin layer of solidified melt. This can be stated when analysing micro hardness values near the interface. The microstructure of parent plates in layers adjacent to the interface is usually composed of fine (sub)grains with a diameter of few hundreds of nanometers (mostly <500 nm). The presence of flattened grains (often of thickness below 100 nm) is detectable. These grains are strongly curved in the vortex region and they reflect very well the rotational character of material displacement during wave formation. It can be also observed that the strain hardening decreases as the distance from the interface increases (Figs. 7c, d).

The presence of melted zones inside the vortexes affects strongly the microstructure of neighbouring severely deformed layers and the values of microhardness significantly drops, independently of the analysed material [15-17, 21]. In these cases thermal softening leads to appearance of new, recrystallized grains, and finally it decreases strength of the entire clad. The formation of new, nearly equiaxed recrystallized grains, which replaced the flattened ones, was observed in Zr700/SS clad, whereas in the Ta/SS clad a layer of columnar grains growing perpendicular to the interface was detected [17].

If melted zones inside the vortex are not observed, only flattened grains dominate the microstructure of the wave crest. By contrast no melted zones are detected at the bottom of the wave, as observed at optical microscopy scale. The dislocation structures in heavily deformed areas shows a tangled network of dislocations. They were composed of roughly elongated cells/(sub)grains with an increased density of dislocations within the (sub)grains. The dimension of elongated cells/(sub)grains depends on the materials. A large number of dislocations accommodated in the cells/(sub)grains strongly indicates that the deformation processes are prevailing over the thermally activated ones, i.e. recovery, recrystallization and grain growth, as suggested earlier for Al/Cu [15,22] and Zr/(carbon steel) [16].

3.3. Low temperature post-processing annealing

Before straitening of the explosively joined sheet the clads are subjected to low temperature annealing leading to release internal stresses. After this process essential microstructural changes are only observed inside the melted zones and in severely deformed layers of the parent plates of low melting point materials.

Changes inside the solidified melt zones. Since annealing temperatures are still higher than those defining the glass temperature transition of given alloy, this process leads to transformation of amorphous phases into fine-grained one. The structural changes are combined with phase transformations and chemical composition changes through the initiation of diffusion processes inside the melted zones during which the non-equilibrium phases are transformed into equilibrium ones.

Changes in parent plates near the interface. The structural changes in severely deformed layers near the interface strongly depends on the melting point of joined metals. It was observed that the severely deformed structure of metals of low melting point (e.g. Al or Mg) undergoes intense recovery and recrystallization, whereas no essential microstructural changes are observed in metals of high melting point.

3.4. High temperature post-processing annealing. Initiation of diffusion process across the interface

The diffusion processes across the interface are dominant for high (and very high) annealing temperatures (as compared to the melting points of joined materials) and for longer annealing times. (Here, high temperature annealing is defined as the process realized at temperatures above which the intense formation of intermetallic layers is observed). In all analysed cases of metal compositions the appearance of new phases and/or the disappearance, growth or transformation of the existing ones was observed.

After a sufficiently long time of high temperature ageing, continuous layers of equilibrium phases (of planar morphology) were formed at the bonded interface. As the ageing time increased these intermetallic phases developed inwards, to the central area, and eventually formed a complete layer between the

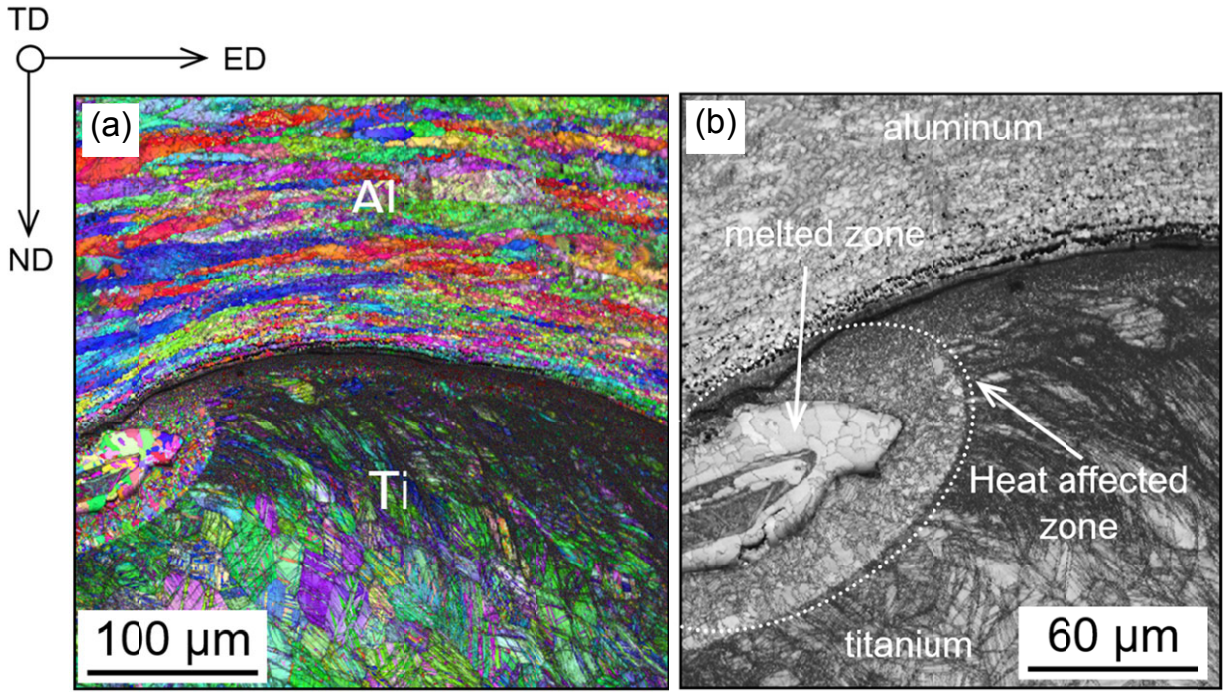

Fig. 9. The influence of large melted zone on the recrystallization of severely deformed areas in Al/Ti clad. (a) SEM/EBSD and (b) image quality images showing formation of the heat affected zone on the wave crest. SEM/EBSD measurements with a step size of 100 nm

bond and pad. The growth kinetics of the intermetallic phases is always diffusion controlled. It is clear that in the conditions close to the equilibrium the chemical composition of the formed phases can be predicted based on the classical phase equilibrium diagrams. Moreover, the sequence of phases is strictly related to the distance from the parent plates, as presented in Fig. 10a for Cu/Ti clad. The phases enriched with Ti were formed close to the Ti plate, whereas the phases enriched with Cu – close to the copper plate. After long time of ageing (here, after 100 h and 1000 h), four intermetallic phases of Ti_2Cu, TiCu, Ti_3Cu_4 and $TiCu_4$ arrayed in the sequence from the Ti to the Cu plate were observed. Since volume fraction of the phases formed near the interface is relatively small, not all of them are visible on X-ray synchrotron diffraction patterns (Fig. 10b). It should be pointed out that the phase sequence observed near the equilibrium conditions, is completely different for that recognized in explosive welding clads (in the as-bonded state).

4. Discussion

4.1. Heat influence

During EXW the rate of heat transfer is one of the most important factors which controls the phase transformations during local melting, solidification of the liquid phase [14-18,23] and structural changes in severely deformed areas of parent sheets/plates [15,23,24]. In this context the EXW process can be divided in two stages. *In the first period*, the heat increase is higher compared with that which can be convected away from areas close to the collision line/point. It is widely accepted that the kinetic energy of the jet, impact energy and the large plastic work, which are dissipated to heat, induce melting of material close to the interface. As the process is very fast, there is no time for the heat to be transferred away, hence temperature increases causing local melting. The calculations made by Guo et al. [25] showed that the heating rate during EXW is of the order of 10^9 K/s, whereas in estimations made by Bataev et al. [14] of the order of 10^7 K/s.

In the second period (as the collision point is moved forward) the melted volumes are subjected to extremely high cooling rates due to good thermal conductivity of metals. It is obvious that the cooling rate changes in different areas substantially not only with time but also with temperature. The temperature model of the explosive bonding given by Yan and Li [26] showed that the cooling rate at the early stage of the bonding is of the order of 10^8 K s^{-1}, whereas after ~20 μs, the cooling rate is close to 10^7 K s^{-1}. Approximately one order of magnitude lower values of cooling rate were estimated by Guo et al. [25] and recently by Bataev et al [14]. Nevertheless, the estimated values are still higher than that required for the formation of an amorphous phase (~10^5 K s^{-1}) allowing the formation of amorphous parts.

Taking into account the above reports it can be established that at the initial stage of the cooling period the cooling rate may vary between 10^6 and 10^8 K/s while after few miliseconds, the cooling rate drops to 10^3-10^4 K/s. It also depends on the thickness of the melted zone. Bataev et al. [14] showed that the cooling rate can reach even 10^9 K/s for very thin regions of the melt. For such cases it is possible to obtain metallic glasses in the vortex zone. Paul et al [16] estimated that for the Zr/carbon steel clad the cooling rate at the beginning stage of the bonding was of the order of 10^8 K s^{-1}, whereas after ~20 μs, it decreases to ~10^7 K s^{-1}. All these changes are accompanied by an intense mixing in the liquid or semi-liquid state powered up by high pressure.

4.2. Changes inside melted zones

The most radical changes are observed inside melted zones during solidification. Depending on the materials used the zones of solidified melt consists of:

(i) stable, crystalline phases that are predicted by equilibrium phase diagrams,

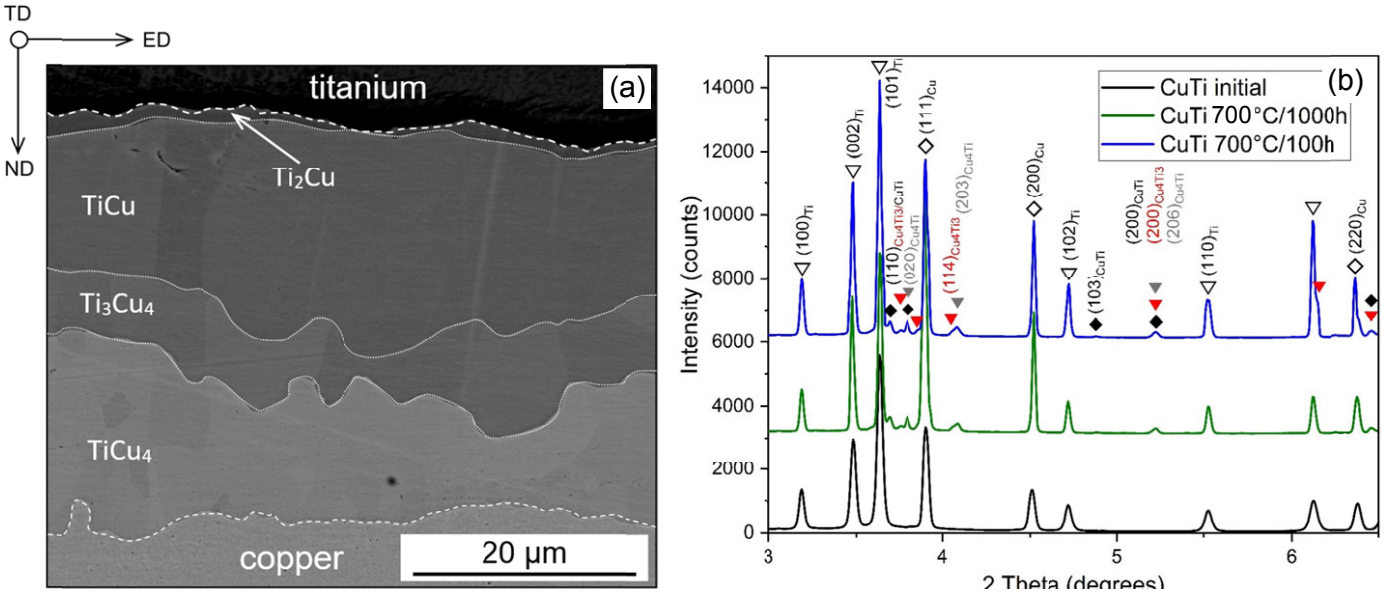

Fi. 10. The intermetallic phases growth during annealing of Cu/Ti clad. Sample annealed at 700°C for 100 h

(ii) metastable, but still crystalline phases that are not observed on equilibrium phase diagrams of given metals composition,
(iii) amorphous, metastable phases, and
(iv) a mixture of various stable and metastable (crystalline and amorphous) phases.

In most observed cases the structures of these zones corresponds to the structures of alloys of the same composition produced by rapid solidification techniques. Thus, one can say that the cooling rate plays a crucial role in amorphous phases formation, which strongly depends on the thickness of the reaction layer.

A thin or extremely thin layers of solidified melt is always formed along the entire contact surface of properly joined plates. Their origin can be twofold. On the one hand the very thin layer can be formed as a result of drag effect of molten or semi-molten material from the large melted zones of open character, as originally discussed by Paul et al. [5]. However, a very thin reaction layer can also be formed on the flat parts of the interface, without any direct contact with the large melted zones. The presence of this extremely thin layer was also documented experimentally in Zr700 to carbon steel [16], Ta to stainless steel [17] and low carbon steel to low carbon steel clads and predicted numerically by Bataev et al. [14]. With this, authors confirm the crucial role of melting in creation of a good quality bond and the validity of hydrodynamic approach [2] for joint formation during EXW.

As a next, it was showed that for low temperature annealing and for short annealing times the essential changes were observed only inside the melted zones. Since annealing temperatures are usually higher than that define for the glass transition of a given alloy, then the transformation of amorphous phases into fine-grained one have to be observed. Another important observation was that after annealing all metastable phases are transformed into stable one, i.e. observed on equilibrium phase diagrams. Their exact chemical composition strongly depends on the annealing conditions.

In all analysed cases of metal compositions the appearance of new phases and/or the disappearance, growth or transformation of the existing ones was observed after long term annealing at high temperatures. The phases formed have always a character of continuous layer(s). It was observed that chemical composition of these phases can be predicted based on the classical phase equilibrium diagrams and the sequence of these phases is strictly related to the distance from the parent plates.

4.2. Changes in severely deformed layers of parent plates

The evolution of microstructure in severely deformed layers of the parent sheets strongly depends on the melting point of joined metals. (The melting point of material determines the occurrence of recovery and recrystallization processes). During clad formation the recrystallization occurs as a result of the heat transfer between the large melted zones and severely deformed layers of parent sheets/plates. This process leads to transformation of elongated dislocation structures (micro bands) in layers near the interface with randomly distributed dislocations inside them into equiaxed fully recrystallized grains [17]. Since the highest temperature is 'located' at the interface, it is very often observed that the grains, which are adjacent to the interface undergo abnormal grain growth. This leads to the situation where the average size of grains situated at the interface is larger than that of more distant from the interface [24].

The influence of defect density and brittle solidified melt zones on the clad strength seems to be rather complex to analyse. Although, the zones of solidified melt exhibit very high hardness as compared to hardness of joined sheets, the recrystallized structure near the interface and easy cracks propagation inside the melted zone can compensate the overall clad strength. It is well documented that the strain hardening of the adjacent interface layers is considered to increase the strength properties of the clad [1,2,7]. This can be attributed to the increase of lattice defects, such as dislocations, vacancies and/or (sub)grain boundaries. However, the recovery and recrystallization processes initiated during EXW can decrease the density of structural defects [27,28] in layers near the interface due to heat transfer from large melted zones towards severely deformed layers. This in turn, leads to decrease of strength.

5. Conclusions

This work describes the microstructure and the chemical composition of the interfacial layers of an explosively welded clads for various metal compositions. The application of the SEM and TEM methods allowed to characterize in detail the structure of the reaction layer and parent layers, which were severely deformed. The following conclusions can be drawn:

(i) During solidification the melted alloys exhibit a strong tendency to form brittle crystalline, nano-grained or amorphous phases of high hardness. It was found that independently of analysed clad most of the phases formed in the melting zones do not appear in the equilibrium phase diagrams.
(ii) For all the analysed metal compositions strong metallurgical bonding was achieved along the whole melting surface of the explosively welded sheets. The above proves that the proper explosive welding always incorporates the melting of a thin interfacial layer between joined materials.
(iii) The interfacial layers of bonded metals are subjected to severe plastic deformation forming nano-grained structures. It was found that this microstructure can undergo dynamic recovery and recrystallization just during clad processing. This led to the formation of recrystallized grains in layers near the interface.
(iv) The structure of the joint subjected to further heat treatment changes substantially. In the case of low temperature annealing (and for short annealing times) the essential changes were only observed inside the melted zones and in severely deformed layers of parent metals of low melting point, whereas the diffusion processes

across the interface are dominant for high temperature annealing and for longer annealing times. The phases formed during annealing always have the character of continuous diffusion layer(s) and their chemical composition corresponds to those observed on the classical phase equilibrium diagrams of given metal composition.

Acknowledgements

This work was supported by the Polish National Centre of Science (NCN), project no.: UMO-2016/21/B/ST8/00462. The authors would like to take this opportunity to express their appreciation.

REFERENCES

[1] T.Z. Blazynski (ed.): Explosive Welding, Forming and Compaction, Applied Science Publishers LTD, New York (1983).

[2] B. Crossland, Explosive welding of metals and its application, Clarendon Press Oxford (1982).

[3] V.I. Lysak, S.V. Kuzmin, Explosive welding of metal layered composite materials. In: Paton BE, editor. Ukraine. Kiev: E.O. Paton Electric Welding Institute (2003).

[4] F. Findik, Recent developments in explosive welding, Mater. Des. **32**, 1081-1093 (2011).

[5] H. Paul, W. Skuza, R. Chulist, M. Miszczyk, A. Gałka, M. Prażmowski, J. Pstruś, The effect of detonation velocity and stand-off distance on the interface morphology and electro-mechanical properties of Ti/Cu clad composites produced by explosive welding, Metall. Mater. Trans. A (2019) submitted.

[6] R. Mendes, B. Ribeiro, A. Loureiro, Effect of explosive characteristics on the explosive welding of stainless steel to carbon steel in cylindrical configuration, Mater. Des. **51**, 182-192 (2013).

[7] A. Durgutlu, B. Gulenc, F. Findik, Examination of copper/stainless steel joints formed by explosive welding, Mater. Des. **26** (6), 497-507 (2005).

[8] Z. Livne, A. Munitz, Characterization of explosively bonded iron and copper plates, J. Mat. Sci. **22**, 1495-1500 (1987).

[9] A. Durgutlu, H. Okuyucu, B. Gulec, Investigations of effect of stand-off distance on interface characteristics of explosively welded copper and stainless steel, Mater. Des. **29**, 1480-1484 (2008).

[10] N. Kahraman, N. Gulec, F. Findik, Joining of titanium/stainless steel and effect on interface, J. Mat. Proc. Technol. **171**, 241-249 (2005).

[11] N. Kahraman, B. Gülenç, Microstructural and mechanical properties of Cu-Ti plates bonded through explosive welding process, J. Mater. Proc. Techn. **169**, 67-71 (2005).

[12] D. Fronczek, J. Wojewoda-Budka, R. Chulist, A. Sypień, A. Kornewa, Z. Szulc, N. Schell, P. Zieba, Structural properties of Ti/Al clads manufactured by explosive welding and annealing, Mater. Des. **91**, 80-89 (2016).

[13] D.V. Lazurenko, I.A. Bataev, V.I. Mali, A.A. Bataev, Iu.N. Milutina, V.S. Lozhlin, M.A. Esikov, A.M.J. Jorge, Explosively welded multilayer Ti-Al composite: Structure and transformation during heat treatment, Mater. Des. **102**, 122-130 (2016).

[14] I.A. Bataev, D.V. Lazurenko, S. Tanaka, K. Hokamoto, A.A. Bataev, Y. Guo, A.M. Jorge Jr., High cooling rates and metastable phases at the interfaces of explosively welded materials, Acta Mater. **135**, 277-289 (2017).

[15] H. Paul, L. Lityńska-Dobrzyńska, M. Prażmowski, Microstructure and phase constitution near the interface of explosively welded aluminium/copper plates, Metall. Mater. Trans. A **44A**, 3836-3851 (2013).

[16] H. Paul, J. Morgiel, M. Faryna, M. Prażmowski, M. Miszczyk, Microstructure and interfacial reactions in the bonding zone of explosively welded Zr700 and carbon steel plates, Int. J. Mater. Res. **106** (7), 782-792 (2015).

[17] H. Paul, M.M. Miszczyk, R. Chulist, M. Prażmowski, J. Morgiel, A. Gałka, M. Faryna, F. Brisset, Microstructure and phase constitution in the bonding zone of explosively welded tantalum and stainless steel sheets, Mater. Des. **153**, 177-189 (2018).

[18] J. Song, A. Kostka, M. Veehmayer, D. Raabe, Hierarchical microstructure of explosive joints: Example of titanium to steel cladding, Mater. Sci. Eng. A **528A**, 2641-2647 (2011).

[19] H. Paul, M. Faryna, M. Prażmowski, R. Banski, Changes in the bonding zone of explosively welded sheets, Arch. Metall. Mater. **56**, 463-474 (2011).

[20] R. Chulist, L. Straka, A. Sozinov, T. Lippmann, W. Skrotzki, Modulation re-orientation in 10M Ni-Mn-Ga martensite, Scripta Mater. **68**, 671-674 (2013).

[21] B. Wronka, Testing of explosive welding and welded joints: joint mechanism and properties of explosive welded joints, J. Mater. Sci. **45**, 4078-40-83 (2010).

[22] Paul, H., Miszczyk, M., Prazmowski, M. Experimental investigation of texture gradients in aluminium/copper plates bonded through explosive welding process, Mater. Sci. Forum **702-703**, 603-606 (2012).

[23] H. Paul, J. Morgiel, T. Baudin, F. Brisset, M. Prażmowski, M. Miszczyk, Characterization of Explosive Weld Joints by TEM and SEM Orientation Imaging Microscopy, Arch. Metall. Mater. **59**, 1129-1136 (2014).

[24] Q. Chu, M. Zhang, J. Li, Ch. Yan, Experimental and numerical investigation of microstructure and mechanical behaviour of titanium/steel interface prepared by explosive welding, Mater. Sci. Eng. A **689**, 323-331 (2017).

[25] Y. Guo, G. Liu, H. Jin, Z. Shi, G. Qiao, Intermetallic phase formation in diffusion-bonded Cu/Al laminates, J. Mater. Sci. **46**, 2467-2473 (2011).

[26] H.H. Yan, X.Y. Li, Theoretical explanation for amorphous phase emerging across the interface during explosive welding, Rare Met. Mater. Eng. **32**, 176-178 (2003).

[27] M.M. Miszczyk, H. Paul, J.H. Driver, P. Drzymała, Recrystallization nucleation in stable aluminium-base single crystals: Crystallography and mechanisms, Acta Mater. **125**, 109-124 (2017).

[28] M.M. Miszczyk, H. Paul, J.H. Driver, J. Poplewska, The influence of deformation texture on nucleation and growth of cube grains during primary recrystallization of AA1050 alloy, Acta Mater. **129**, 378-387 (2017).